



# Development of Red Exciplex for Efficient OLEDs by Employing a Phosphor as a Component

Ming Zhang<sup>1,2†</sup>, Kai Wang<sup>2†</sup>, Cai-Jun Zheng<sup>1\*</sup>, De-Qi Wang<sup>1</sup>, Yi-Zhong Shi<sup>2</sup>, Hui Lin<sup>1</sup>, Si-Lu Tao<sup>1</sup>, Xing Li<sup>2</sup> and Xiao-Hong Zhang<sup>2\*</sup>

<sup>1</sup> School of Optoelectronic Science and Engineering, University of Electronic Science and Technology of China, Chengdu, China, <sup>2</sup> Institute of Functional Nano & Soft Materials (FUNSOM) and Jiangsu Key Laboratory for Carbon-Based Functional Materials & Devices, Soochow University, Suzhou, China

## OPEN ACCESS

### Edited by:

Lian Duan,  
Tsinghua University, China

### Reviewed by:

Qisheng Zhang,  
Zhejiang University, China  
Toshinori Matsushima,  
Kyushu University, Japan

### \*Correspondence:

Cai-Jun Zheng  
zhengcaijun@uestc.edu.cn  
Xiao-Hong Zhang  
xiaohong\_zhang@suda.edu.cn

<sup>†</sup>These authors have contributed  
equally to this work

### Specialty section:

This article was submitted to  
Organic Chemistry,  
a section of the journal  
Frontiers in Chemistry

Received: 07 November 2018

Accepted: 08 January 2019

Published: 31 January 2019

### Citation:

Zhang M, Wang K, Zheng C-J,  
Wang D-Q, Shi Y-Z, Lin H, Tao S-L,  
Li X and Zhang X-H (2019)  
Development of Red Exciplex for  
Efficient OLEDs by Employing a  
Phosphor as a Component.  
Front. Chem. 7:16.  
doi: 10.3389/fchem.2019.00016

Exciplexes are ideal candidates as effective thermally activated delayed fluorescence (TADF) emitters. However, efficient orange and red TADF exciplexes have been reported seldomly, because their significant non-radiative (NR) decay of excited states lead to unavoidable energy loss. Herein, we propose a novel strategy to construct efficient red TADF exciplexes by introducing phosphor as one component. Due to the strong spin-orbit coupling of heavy metal (e.g., Ir, Pt, et al.) ion cores, the NR decays will be evidently decreased for both singlet and triplet excitons, reducing the undesired exciton waste. Moreover, compared with the conventional exciplexes, phosphorescence plays an important role for such novel exciplexes, further improving the exciton utilization. Based on this strategy, we fabricated a red exciplex containing 1,3,5-triazine-2,4,6-triyl)tris(benzene-3,1-diy)tris(diphenylphosphine oxide) (PO-T2T) and tris(2-phenylpyridine) iridium(III) (Ir(ppy)<sub>3</sub>) as components and realize a red emission with a peak at 604 nm, a CIE coordinate of (0.55, 0.44), and a high maximum external quantum efficiency of 5% in organic light-emitting device. This efficiency is 2.6 times higher than that of the device based on the conventional red exciplex emitter, proving the superiority of our novel strategy to construct TADF exciplexes with phosphors.

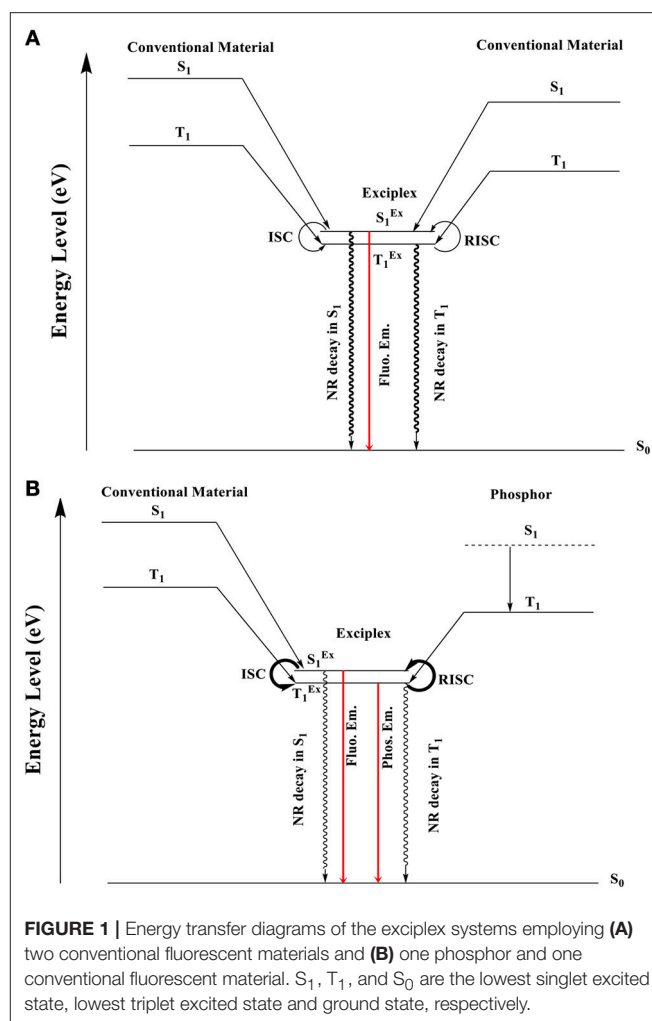
**Keywords:** exciplex, thermally activated delayed fluorescence, phosphor, spin-orbit coupling, non-radiative decay

## INTRODUCTION

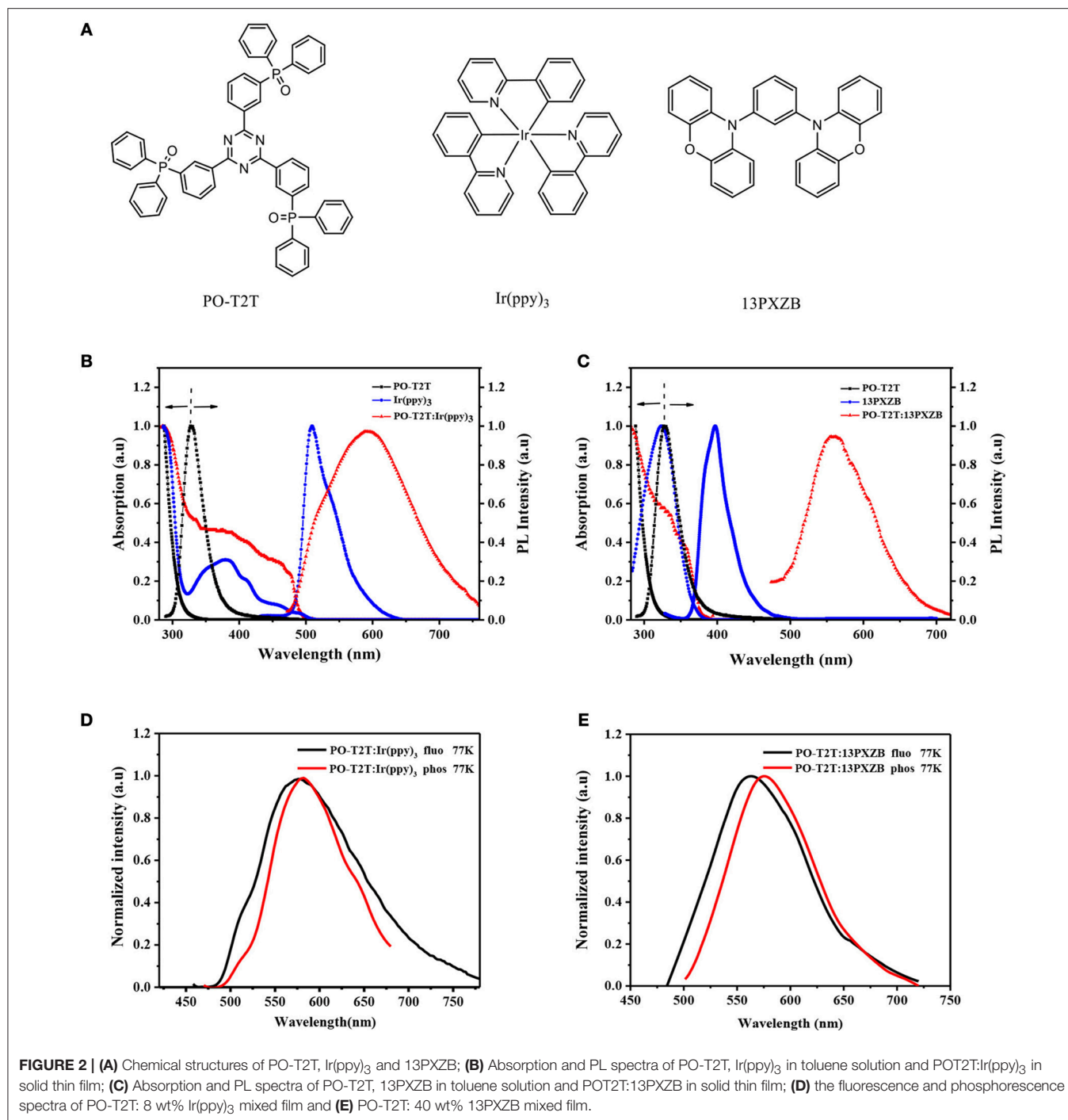
Organic light-emitting devices (OLEDs) based on thermally activated delayed fluorescence (TADF) emitters are considered the new generation of OLEDs (Adachi, 2014) and have drawn great attention in recent years (Goushi et al., 2012; Uoyama et al., 2012; Zhang et al., 2014b, 2016; Ban et al., 2015; Hirata et al., 2015; Liu M. et al., 2015, 2017; Liu W. et al., 2015; Chen et al., 2016, 2017; Gómez-Bombarelli et al., 2016; Li et al., 2016, 2017, 2018; Xie et al., 2016; Miwa et al., 2017; Moon et al., 2017; Shiu et al., 2017; Wang K. et al., 2017a; Yang et al., 2017). The TADF emitters can utilize both singlet and triplet excitons for emission by up-converting non-radiative (NR) triplet excitons to radiative singlet excitons via an efficient reverse intersystem crossing (RISC) process from lowest triplet state ( $T_1$ ) to lowest singlet state ( $S_1$ ) (Uoyama et al., 2012). Theoretically, an effective RISC process requires that the TADF emitter possesses an extremely small singlet-triplet energy splitting ( $\Delta E_{ST}$ ) between  $S_1$  and  $T_1$  (Uoyama et al., 2012), which needs to isolate its highest occupied molecular

orbital (HOMO) and lowest unoccupied molecular orbital (LUMO) (Chen et al., 2016; Wang D. Q. et al., 2017; Wang et al., 2017b). Clearly, exciplexes are among the ideal candidates as effective TADF emitters, because they meet the requirements mentioned above naturally (Liu et al., 2015a,b, 2016). Formed via intermolecular charge-transfer (CT) transition, the HOMOs and LUMOs of exciplexes are independently located on the electron-donor (D) and electron-acceptor (A) component molecules respectively, possessing extremely small overlaps. Thus, exciplex systems present extremely small energy gaps between their own  $^1\text{CT}$  and  $^3\text{CT}$  ( $<0.1\text{ eV}$ ). By using high- $T_1$  component molecules to avoid the triplet excitons loss, exciplexes commonly exhibit TADF characteristics. In the past few years, great progress has been made for exciplex-based TADF OLEDs (Goushi et al., 2012; Li et al., 2014; Liu et al., 2015b,c, 2016; Zhang et al., 2017; Shi et al., 2018). In 2012, Adachi and co-workers firstly reported a yellow-green TADF exciplex, and theoretically proved its great potential (Goushi et al., 2012). In 2015, our group developed a novel strategy to predict and design efficient exciplex with TADF characteristics by using the HOMO and LUMO energy levels of constituting molecules (Liu et al., 2015a). And in 2016, our group further reported highly efficient exciplex-based TADF OLED with an high external quantum efficiency (EQE) of 17.8% (Liu et al., 2016). However, nearly all the currently reported exciplex TADF emitters are limited in short-wavelength (i.e., blue, green, and yellow) emission (Goushi et al., 2012; Li et al., 2014; Liu et al., 2015b,c, 2016; Zhang et al., 2017; Shi et al., 2018). Efficient TADF exciplexes with long-wavelength (i.e., orange and red) emission have rarely been reported (Data et al., 2016). **Figure 1A** illustrates the exciton transfer processes in conventional TADF exciplexes. Both the constituting molecules should have higher  $S_1$  and  $T_1$  energy levels than that of exciplex, ensuring all excitons can be harvested on  $S_1$  and  $T_1$  states of exciplex (Liu et al., 2015a). Therefore, the energy loss of the exciplex-based TADF OLEDs should be mainly caused by the NR decay of both exciplex  $S_1$  and  $T_1$  states. According to photophysical theory, the rate constants of the NR decays are exponentially magnified with the decreased bandgap energy level (Zhang et al., 2014a). For TADF exciplexes with short-wavelength emission, the NR decays of  $S_1$  and  $T_1$  states are almost neglectful compared with the emission process of  $S_1$  state and RISC process of  $T_1$  state, realizing high exciton utilization in the OLEDs (Liu et al., 2016). While for common orange and red TADF exciplexes, the NR decays of excited states become significant due to narrow bandgaps, leading to unavoidable energy loss. Therefore, efficient orange and red TADF exciplexes are hard to be achieved by these common exciplex systems and become the bottleneck of exciplexes development.

In this study, we proposed a novel strategy to construct efficient red exciplexes by introducing a phosphor as one component. As we known, phosphors are generally heavy metal complexes. The spin-orbit coupling (SOC) of heavy metal (Ir, Pt, et al.) ion cores will significantly enhance the energy transfer processes between singlet and triplet states [intersystem crossing process (ISC) from  $S_1$  to  $T_1$  and phosphorescent decay from  $T_1$  to  $S_0$ ], allowing heavy metal complexes to achieve phosphorescence efficiently (Baldo et al., 1998; Liu X.



et al., 2015; Liu B. et al., 2017). Correspondingly, in new type exciplexes, the decay routes of excited exciplexes will be also affected by the heavy metal phosphor cores. The ISC process from  $S_1^{\text{EX}}$  to  $T_1^{\text{EX}}$ , RISC process from  $T_1^{\text{EX}}$  to  $S_1^{\text{EX}}$  and phosphorescent decay from  $T_1^{\text{EX}}$  to  $S_0^{\text{EX}}$  can be significantly enhanced by the SOC effect. Thus, the proportions of the NR decays will be accordingly decreased for  $S_1^{\text{EX}}$  and  $T_1^{\text{EX}}$  states, reducing the undesired exciton waste. Moreover, compared with the conventional exciplexes, phosphorescence may play an important role on such new type of exciplexes with phosphor (Cherpak et al., 2015) (**Figure 1B**), further improving the exciton utilization. Based on this novel strategy, we fabricated a red exciplex containing 1,3,5-triazine-2,4,6-triyl)tris(benzene-3,1-diyl)tris(diphenylphosphine oxide) (PO-T2T) and tris(2-phenylpyridine) iridium(III) ( $\text{Ir}(\text{ppy})_3$ ) as components, which exhibits typical TADF characteristic with an extremely small  $\Delta E_{\text{ST}}$  of 0.026 eV. In device, PO-T2T: $\text{Ir}(\text{ppy})_3$  exciplex shows a red emission with a peak at 604 nm and a CIE coordinate of (0.55, 0.44), and realizes a high maximum external quantum efficiency (EQE) of 5%. As a comparison, the conventional TADF exciplex consisting of PO-T2T and 1,3-di(10H-phenoxazin-10-yl)benzene (13PXZB) only achieves a maximum EQE of 1.9% in



device. These results not only demonstrate exciplexes can also be formed by using a phosphor component, but also indicate that the NR decays of excited states can be significantly suppressed for phosphor-based exciplexes by the SOC effect of heavy metal ion core from phosphor. Although noble metal Ir is contained in our system, we believe efficient but low-cost phosphor-based exciplex emitters can be developed by using other cheap heavy metal-based phosphors, like Cu, et al.

## RESULTS AND DISCUSSION

**Figure 2A** illustrates the molecular structures of PO-T2T, Ir(ppy)<sub>3</sub> and 13PXZB. PO-T2T and Ir(ppy)<sub>3</sub> were directly purchased from commercial sources, and 13PXZB was newly designed and synthesized as shown in **Supporting Information**. The cyclic voltammograms of the three materials are shown in **Figure S1**. Both Ir(ppy)<sub>3</sub> and 13PXZB show nearly identical

oxidation onsets, and their HOMO energy levels are accordingly estimated to be identically at  $-5.30$  eV, while the LUMO energy level of PO-T2T is estimated to be  $-3.26$  eV from the onset of the reduction curve. Combining the energy gaps determined from the onsets of absorption spectra, the LUMO energy levels are estimated to be  $-2.76$  eV for Ir(ppy)<sub>3</sub> and  $-1.95$  eV for 13PXZB, and the HOMO energy level of PO-T2T is  $-6.93$  eV. Based on our previous study, the driving force for exciplex formation can be approximately described as Equation (1) (Liu et al., 2015a)

$$\begin{aligned} -\Delta G_{\text{EX}} &= \text{HOMO}_{\text{D}} - \text{HOMO}_{\text{A}}(\text{for acceptor}) \text{ or} \\ -\Delta G_{\text{EX}} &= \text{LUMO}_{\text{D}} - \text{LUMO}_{\text{A}}(\text{for donor}) \end{aligned} \quad (1)$$

Thus, the driving forces are approximately estimated to be  $1.63$  eV for PO-T2T and  $0.5$  eV for Ir(ppy)<sub>3</sub> in the PO-T2T:Ir(ppy)<sub>3</sub> system and  $1.63$  eV for PO-T2T and  $1.31$  eV for 13PXZB in the PO-T2T:13PXZB system. These high values can ensure the exciplex formation in both systems. Moreover, as the CT transition of exciplex happens between LUMO of A and HOMO of D, the exciplex energy can be described as Equation (2), where the constant is exciton binding energy and ranges from 0 to  $0.20$  eV (Kolosov et al., 2002)

$$E_{\text{exciplex}} = e(\text{LUMO}_{\text{A}} - \text{HOMO}_{\text{D}}) + \text{constant} \quad (2)$$

Thus, both exciplexes possess energy of  $2.02$  eV approximately, ensuring they exhibit red emission. Moreover, the respective T<sub>1</sub> energy levels of PO-T2T, Ir(ppy)<sub>3</sub> and 13PXZB are  $2.95$ ,  $2.45$ , and  $2.73$  eV, which are determined from the highest energy vibronic sub-band of their phosphorescence spectra at  $77$  K (Figure S2). These T<sub>1</sub> energy values of components are much higher than both exciplex energies, which boosts the exciplex to harvest all excitons.

The absorption and photoluminescence (PL) spectra of PO-T2T:Ir(ppy)<sub>3</sub> and PO-T2T:13PXZB exciplexes were investigated first. As shown in Figures 2B,C, the absorption spectra of both PO-T2T:Ir(ppy)<sub>3</sub> and PO-T2T:13PXZB mixed films are nearly identical to their constituting molecules at room temperature, suggesting that there are no extra transitions generated in the ground states. Correspondingly, their PL spectra show broad emissions in the range of  $480$ – $733$  nm with a peak at  $590$  nm for PO-T2T:Ir(ppy)<sub>3</sub> and in the range from  $480$  to  $670$  nm with a peak at  $562$  nm for PO-T2T:13PXZB, which significantly differ from the PL spectra of the individual constituting molecules, proving the formation of exciplexes for both films during the photoexcitations. And the PL spectrum of PO-T2T:Ir(ppy)<sub>3</sub> is slightly red-shifted compared with that of PO-T2T:13PXZB, indicating PO-T2T:13PXZB actually has higher energy than PO-T2T:Ir(ppy)<sub>3</sub>. Particularly, in the PL spectrum of PO-T2T:Ir(ppy)<sub>3</sub> mixed film, a slight shoulder can be observed at

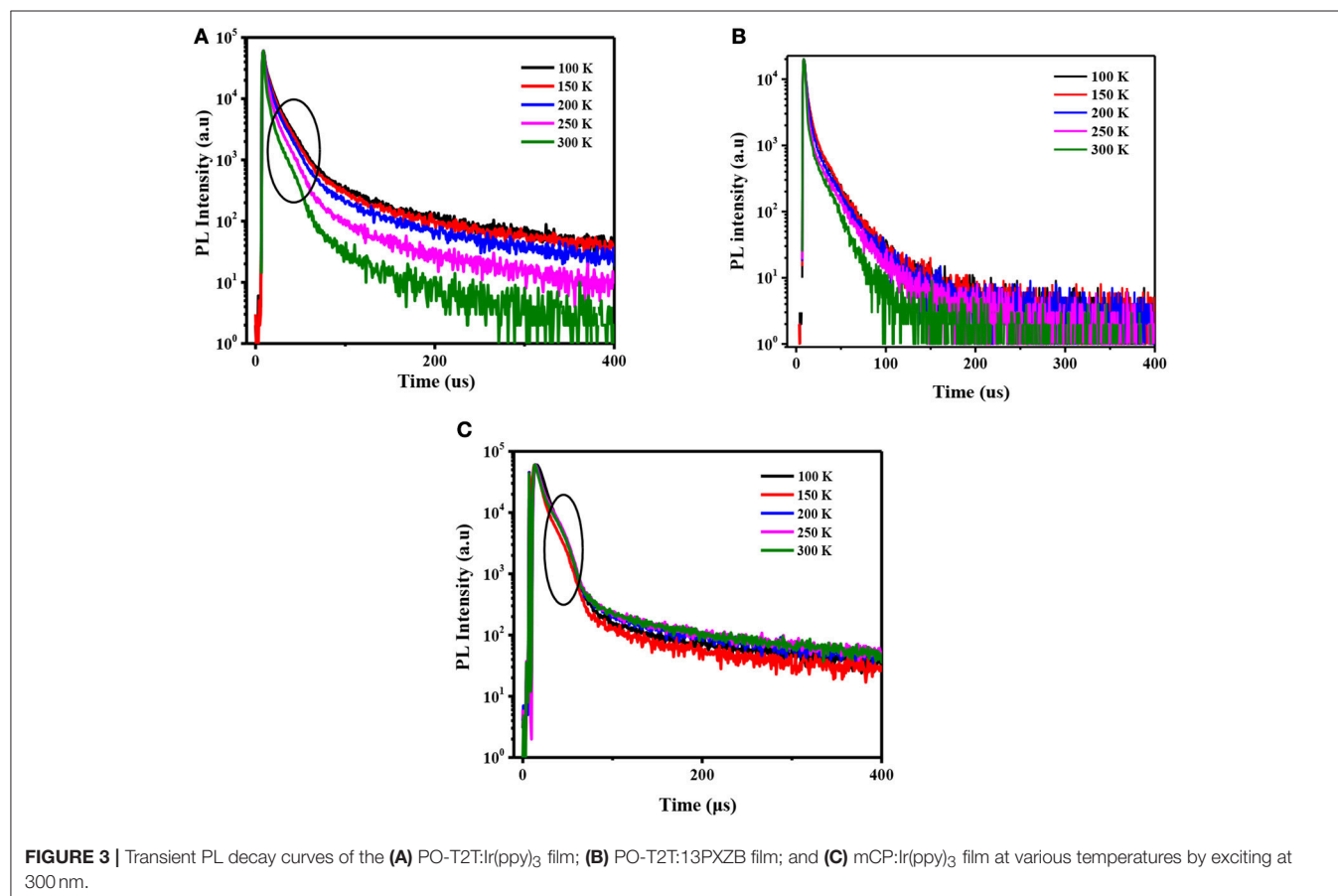
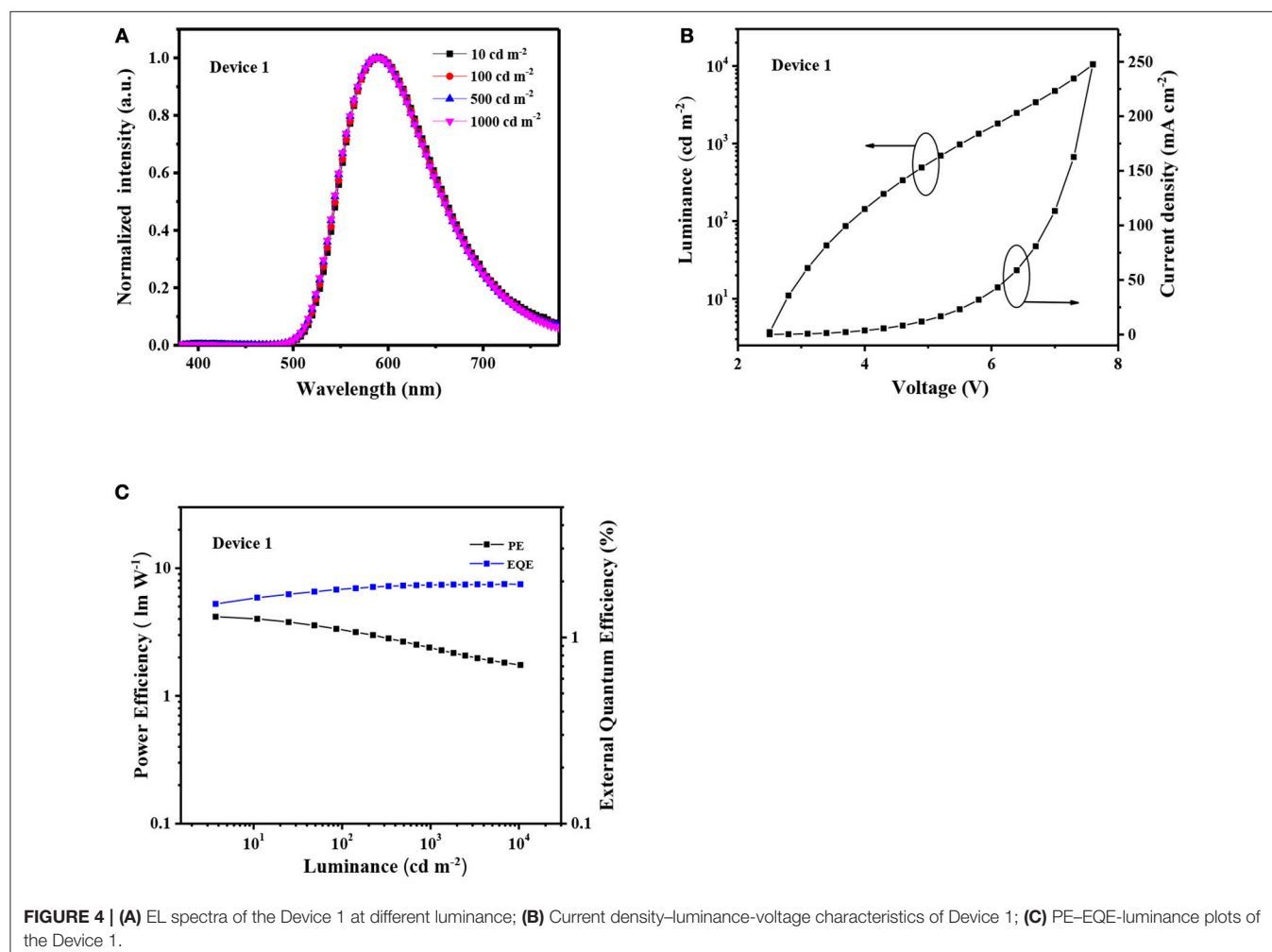


**FIGURE 3** | Transient PL decay curves of the (A) PO-T2T:Ir(ppy)<sub>3</sub> film; (B) PO-T2T:13PXZB film; and (C) mCP:Ir(ppy)<sub>3</sub> film at various temperatures by exciting at  $300$  nm.

the emission area of Ir(ppy)<sub>3</sub>, suggesting that the original metal-to-ligand CT transition of Ir(ppy)<sub>3</sub> is still competitive during the photoexcitation.

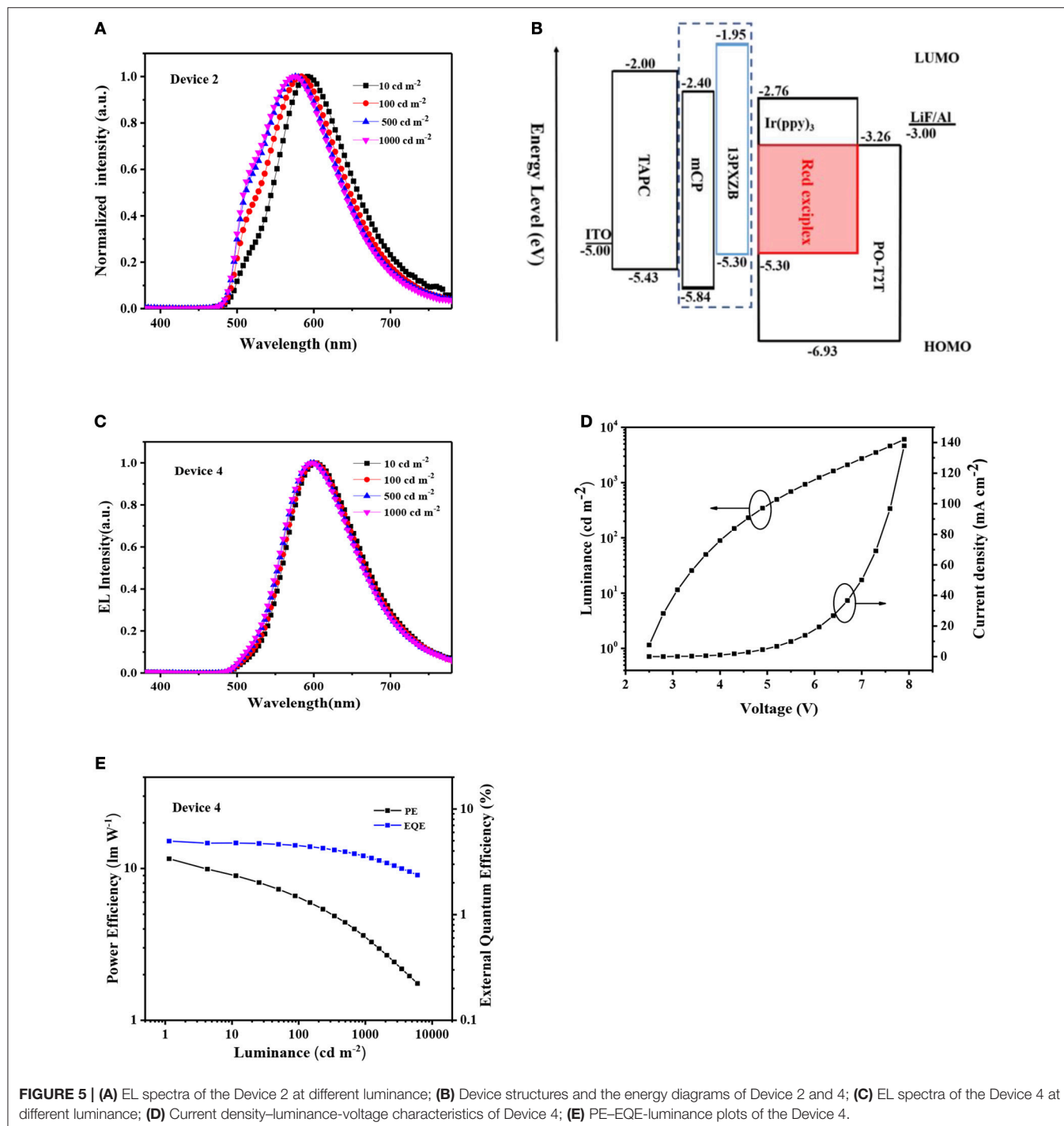
To study the photophysical properties of both exciplexes, we further measured the fluorescence and phosphorescence spectra of the two mixed films at 77 K. As shown in **Figures 2D,E**, from the peaks in the fluorescence and phosphorescence spectra, the S<sub>1</sub> and T<sub>1</sub> energy levels of both the exciplex systems were estimated to be 2.162 and 2.136 eV for PO-T2T:Ir(ppy)<sub>3</sub> and 2.215 and 2.188 eV for PO-T2T:13PXZB, respectively. Thus, their  $\Delta E_{ST}$ s are calculated to be 0.026 and 0.030 eV for PO-T2T:Ir(ppy)<sub>3</sub> and PO-T2T:13PXZB, respectively. These extremely small  $\Delta E_{ST}$ s can lead to efficient RISC process from T<sub>1</sub> to S<sub>1</sub> state, which endow both exciplexes with TADF characteristic. Temperature-dependent transient decay characteristics of these two exciplexes were further measured under nitrogen atmosphere. As shown in **Figure 3** and **Figure S3**, by exciting both the components at 300 nm, the lifetimes of both PO-T2T:Ir(ppy)<sub>3</sub> and PO-T2T:13PXZB exciplexes show significantly decline along with the temperature increasing from 100 to 300 K, indicating their TADF characteristics. At room temperature, PO-T2T:Ir(ppy)<sub>3</sub> shows a

prompt lifetime of 13.2 ns and extremely small delayed lifetime of 2.8  $\mu$ s. PO-T2T:13PXZB exciplex has a prompt lifetime of 17.1 ns and a decay lifetime of 13.9  $\mu$ s, which is significantly longer than that of PO-T2T:Ir(ppy)<sub>3</sub> film. This phenomenon is caused by the SOC effect of heavy metal core in phosphor, which can effectively enhance the RISC process. Moreover, in the range of <100  $\mu$ s (shown in **Figures 3A,C**), significant turning curves can be observed with a similar behavior compared to the initial curve of Ir(ppy)<sub>3</sub>, which should indicate the evident contribution of exciplex phosphorescence. PL quantum yields (PLQYs) of PO-T2T:Ir(ppy)<sub>3</sub> and PO-T2T:13PXZB mixed films with a thin thickness of 5 nm were measured via integrating sphere measurements in atmosphere. Both films present a similar low PLQY value of about 4%. Considering that most of triplet excitons can be quenched by oxygen, the PLQY value will be mainly contributed by the prompt component of singlet excitons, and both of the exciplexes should have similar luminescence efficiencies in the devices if we neglect the effect of triplet excitons (M  hes et al., 2012). While under oxygen-free condition, both singlet and triplet excitons make contributions to the emission. As a result, the PLQY values were increased to 23.3 and 8.6%



for PO-T2T:Ir(ppy)<sub>3</sub> and PO-T2T:13PXZB, respectively at room temperature. The evidently higher PLQY of PO-T2T:Ir(ppy)<sub>3</sub> should be ascribed to the reduced NR decays of excited states. To further understand this point, PL spectra and delayed transient PL decays at various temperatures were measured and shown in **Figure S4**, and the data are extracted and summarized in **Table S1**. Different from conventional TADF emitters, the PL intensities are decreased from 200 to 300 K for both exciplexes.

This result is because NR decays are significantly enhanced with the increased temperatures. The triplet formation efficiency ( $\Phi_T$ ) and  $\Delta E_{ST}$  were derived using a Berberan-Santos plot from the temperature-dependent results (in the **Supporting Information**) (Berberan-Santos and Garcia, 1996; Wang H. et al., 2014). The intersystem crossing rate constant ( $k_{ISC}$ ), the non-radiative rate of singlet excitons constants ( $k_{nr}^S$ ) and the non-radiative of triplet excitons rate constant ( $k_{nr}^T$ ) were also calculated assuming



that  $k_{ISC}$  was independent of temperature, and summarized in **Table S2**. The  $k_{ISC}$  of PO-T2T:Ir(ppy)<sub>3</sub> and PO-T2T:13PXZB were calculated to be  $6.70 \times 10^7$  and  $4.93 \times 10^7$  s<sup>-1</sup>. Meanwhile, the  $k_{nr}^S$  of PO-T2T:Ir(ppy)<sub>3</sub> and PO-T2T:13PXZB were calculated to be  $0.73 \times 10^7$  and  $0.85 \times 10^7$  s<sup>-1</sup>. Moreover, the  $k_{nr}^T$  of the PO-T2T:Ir(ppy)<sub>3</sub> and PO-T2T:13PXZB were estimated to  $7.00 \times 10^3$  and  $1.04 \times 10^4$  s<sup>-1</sup>, respectively. Obviously, the  $k_{nr}^S$  and  $k_{nr}^T$  of PO-T2T:Ir(ppy)<sub>3</sub> are lower than the PO-T2T:13PXZB, proving the NR decays of S<sub>1</sub> and T<sub>1</sub> states are suppressed in phosphor-based exciplexes.

To evaluate the electroluminescence (EL) performance of the two exciplex, both PO-T2T:Ir(ppy)<sub>3</sub> and PO-T2T:13PXZB exciplexes were used as the emitters to fabricate the devices, respectively. Due to the excellent electron transporting property of PO-T2T and good hole transporting property of 13PXZB (as shown in **Figure S5**), the PO-T2T:13PXZB-based device is constructed with a structure of ITO/TAPC (35 nm)/13PXZB (10 nm)/PO-T2T:x wt% 13PXZB (30 nm)/PO-T2T (45 nm)/LiF (1 nm)/Al (100 nm) (Device 1). In the device, cyclohexylidenebis[*N,N*-bis(4-methylphenyl)aniline] (TAPC) and PO-T2T are respectively used as the hole-transporting layer (HTL) and electron-transporting layer, ITO (indium tin oxide) and LiF/Al work as the anode and the cathode, respectively. A thin layer of 10 nm 13PXZB is inserted between HTL and the emitting layer (EML) aiming to avoid additional exciplex formed between TAPC and PO-T2T. The doping concentration of 13PXZB in EML is optimized to 40 wt% for Device 1. As shown in **Figure 4**, Device 1 exhibits a low turn-on voltage (at the brightness of 1 cd m<sup>-2</sup>) of 2.5 V and stable red EL emission at different luminances with a peak at 592 nm and a CIE coordinate of (0.52, 0.47), indicating that we have successfully constructed a red exciplex with a conventional material system of PO-T2T and 13PXZB. However, the maximum current efficiency (CE), power efficiency (PE), and EQE of Device 1 are only 4.2 cd A<sup>-1</sup>, 2.0 lm W<sup>-1</sup> and 1.9%, respectively. Such low device efficiency should be ascribed to the evident NR decays of S<sub>1</sub> and T<sub>1</sub> states for conventional red exciplexes.

Different from PO-T2T:13PXZB exciplex, both PO-T2T and Ir(ppy)<sub>3</sub> are electron transporting materials. As shown in **Figure S5**, the electron transporting capacity of PO-T2T:Ir(ppy)<sub>3</sub> is significantly better than its hole transporting capacity. Thus, an electron-blocking layer (EBL) is needed to benefit carrier recombination in the device. We first constructed Device 2 with a structure of ITO/TAPC (35 nm)/mCP (10 nm)/PO-T2T:x wt% Ir(ppy)<sub>3</sub> (30 nm)/PO-T2T (45 nm)/LiF (1 nm)/Al (100 nm). 3-bis(9H-carbazol-9-yl)benzene (mCP) is used as EBL due to its unipolar hole transporting capacity. And the doping concentration of Ir(ppy)<sub>3</sub> is optimized to 8 wt%. However, as shown in **Figure 5A**, Device 2 exhibits unsatisfactory EL spectra with additional green emission around 520 nm which should be attributed to the phosphorescence of the initial Ir(ppy)<sub>3</sub>. This phenomenon is consistent with the PL spectrum as shown in **Figure 2B**, indicating competition of exciton harvest between Ir(ppy)<sub>3</sub> and PO-T2T:Ir(ppy)<sub>3</sub>. In Device 2, the excitons are generated at the interface of mCP/PO-T2T:Ir(ppy)<sub>3</sub>. Beyond PO-T2T:Ir(ppy)<sub>3</sub>, the excited states of mCP:PO-T2T exciplex

is also unavoidably generated. The energy of mCP:PO-T2T exciplex is around 2.63 eV (Liu et al., 2016), higher than the energies of Ir(ppy)<sub>3</sub> and PO-T2T:Ir(ppy)<sub>3</sub>. The competition between Ir(ppy)<sub>3</sub> and PO-T2T:Ir(ppy)<sub>3</sub> should be led by the energy transfers from mCP:PO-T2T to Ir(ppy)<sub>3</sub> and PO-T2T:Ir(ppy)<sub>3</sub>.

To avoid the harmful green emission, the exciton harvest of Ir(ppy)<sub>3</sub> should be suppressed. Thus, we designed an optimized a device structure by changing mCP EBL to 13PXZB. At the 13PXZB/PO-T2T:Ir(ppy)<sub>3</sub> interface, the excited states of PO-T2T:13PXZB can also generate. But the energy of PO-T2T:13PXZB is in between that of Ir(ppy)<sub>3</sub> and PO-T2T:Ir(ppy)<sub>3</sub>, which can prevent the exciton harvest of Ir(ppy)<sub>3</sub> and thus suppress the green emission. To further prove this point, we also fabricated a device with a structure of ITO/TAPC (35 nm)/13PXZB (10 nm)/PO-T2T (75 nm)/LiF (1 nm)/Al (100 nm) (Device 3). As shown in **Figure S6**, Device 3 exhibits the same EL spectra compared with Device 1 and slightly lower maximum efficiencies of 3.5 cd A<sup>-1</sup> for CE, 2.9 lm W<sup>-1</sup> for PE and 1.6% for EQE. The reason is that Ir(ppy)<sub>3</sub> cannot harvest the excitons from the red exciplex PO-T2T:13PXZB.

Thus, for PO-T2T:Ir(ppy)<sub>3</sub> exciplex, Device 4 was finally constructed with a structure of ITO/TAPC (35 nm)/13PXZB (10 nm)/PO-T2T:x wt% Ir(ppy)<sub>3</sub> (30 nm)/PO-T2T (45 nm)/LiF (1 nm)/Al (100 nm). And the optimized doping concentration of Ir(ppy)<sub>3</sub> in EML is also 8 wt%. As shown in **Figure 5B**, compared with mCP, 13PXZB also has more appropriate HOMO and LUMO energy levels, which can benefit the hole injection to EML and prevent the electron escape from EML. As shown in **Figure 5C**, a stable red EL emission with a peak at 604 nm and a CIE coordinate of (0.55, 0.44) is successfully generated, and the green emission from Ir(ppy)<sub>3</sub> nearly disappeared in the spectra, indicating the feasibility of our device optimization. As shown in **Figure S7**, the EL spectrum of Device 4 is clearly red-shifted compared with that of Device 1 and 3. Such results indicate that not only the emission is from PO-T2T:Ir(ppy)<sub>3</sub> exciplex, but also effective energy transfer is proved from PO-T2T:13PXZB to PO-T2T:Ir(ppy)<sub>3</sub>. As listed in **Table 1** and shown in **Figures 5C-E**, Device 4 realizes a low turn-on voltage of 2.5 V and maximum CE, PE and EQE of 9.3 cd A<sup>-1</sup>, 11.6 lm W<sup>-1</sup> and 5%, respectively. Such high EQE is 2.6 times and 3.1 times higher than that of Device 1 and 3, respectively. And EQE value of 5% is the highest result for red TADF OLEDs based on exciplex emitters. Considering both PO-T2T:13PXZB and PO-T2T:Ir(ppy)<sub>3</sub> possess the same PLQY value of about 4% under triplet excitons quenched condition, the evident efficiency difference between Device 1, 3, and 4 indicates much higher triplet exciton utilization of PO-T2T:Ir(ppy)<sub>3</sub>, which should be ascribed to the beneficial effect of heavy metal ion core in the phosphor component. The SOC effect of heavy metal ion core can not only effectively suppress the NR decays of excited states for red TADF exciplexes, but also induce phosphorescence and make great contribution to EL emission. Our study provides a novel approach to develop efficient red TADF exciplexes with phosphors.

**TABLE 1** | Summary of performances of the exciplex-based devices.

Device	$V_{\text{On}}^{\text{a}}$ [V]	$\lambda_{\text{MAX}}$ [nm]	CE/PE/EQE <sup>b</sup> [cd A <sup>-1</sup> /lm W <sup>-1</sup> /%]			CIE <sup>c</sup> [x, y]
			Maximum	@ 100 cd m <sup>-2</sup>	@ 1,000 cd m <sup>-2</sup>	
1	2.5	592	4.2/2.0/1.9	3.9/3.4/1.8	4.2/2.4/1.9	(0.52,0.47)
2	2.6	584	21.6/19.4/9.6	21.3/17.6/9.5	16.1/10.1/7.2	(0.48,0.49)
3	2.6	592	3.5/2.9/1.6	3.4/2.3/1.5	3.0/1.3/1.4	(0.52,0.47)
4	2.5	604	9.3/11.6/5.0	8.4/6.6/4.5	6.7/3.6/3.6	(0.55,0.44)

<sup>a</sup>Turn-on voltage, estimated at 1 cd m<sup>-2</sup>; <sup>b</sup>CE, current efficiency; PE, power efficiency; EQE, external quantum efficiency; <sup>c</sup>Estimated at 100 cd m<sup>-2</sup>.

## CONCLUSION

In summary, we present a novel strategy to construct efficient red TADF exciplexes by introducing phosphor as one component. The SOC effect of heavy metal ion core in phosphor can suppress the NR decays of excited states and induced phosphorescence makes great contribution to total emission, thus improving the exciton utilization. Red TADF exciplex PO-T2T:Ir(ppy)<sub>3</sub> is constructed accordingly, which exhibits high maximum efficiencies of 9.3 cd A<sup>-1</sup> CE, 11.6 lm W<sup>-1</sup> PE, and 5% EQE in the device. Such high EQE is 2.6 times higher than that of the device based on the comparative conventional red TADF exciplex PO-T2T:13PXZB and the best performance among reported red TADF OLEDs based on exciplex emitters. These results not only provide a new pathway to develop efficient exciplex emitters with vast phosphors, but also demonstrate the superiority of phosphor-based exciplexes.

## AUTHOR CONTRIBUTIONS

C-JZ and X-HZ designed whole work. MZ, KW, and Y-ZS characterize the physical properties of compounds. MZ, KW,

and HL fabricated and optimized the devices. D-QW and XL synthesized the new organic compound. MZ and KW wrote the paper with support from C-JZ, S-LT, and X-HZ. All authors contributed to the general discussion.

## FUNDING

This work was supported by the National Natural Science Foundation of China (Grant Nos. 51773029, 51373190 and 51533005), the National Key Research & Development Program of China (Grant No. 2016YFB0401002), the Collaborative Innovation Center of Suzhou Nano Science & Technology, the Priority Academic Program Development of Jiangsu Higher Education Institutions (PAPD), and the 111 Project and Qing Lan Project, P. R. China.

## SUPPLEMENTARY MATERIAL

The Supplementary Material for this article can be found online at: <https://www.frontiersin.org/articles/10.3389/fchem.2019.00016/full#supplementary-material>

## REFERENCES

- Adachi, C. (2014). Third-generation organic electroluminescence materials. *Jpn. J. Appl. Phys.* 53:060101. doi: 10.7567/jjap.53.060101
- Baldo, M. A., O'Brien, D. F., You, Y., Shoustikov, A., Sibley, S., Thompson, M. E., et al. (1998). Highly efficient phosphorescent emission from organic electroluminescent devices. *Nature* 395:151. doi: 10.1038/25954
- Ban, X. X., Jiang, W., Sun, K., Yang, H., Miao, Y., Yang, F., et al. (2015). Systematically tuning the  $\Delta$ EST and charge balance property of bipolar hosts for low operating voltage and high power efficiency solution-processed electrophosphorescent devices. *J. Mater. Chem. C*, 3, 5004–5016. doi: 10.1039/c5tc00691k
- Berberan-Santos, M. N., and Garcia, J. M. M. (1996). Unusually Strong Delayed Fluorescence of C70. *J. Am. Chem. Soc.* 118, 9391–9394. doi: 10.1021/ja961782s
- Chen, D. Y., Liu, W., Zheng, C. J., Wang, K., Li, F., Tao, S. L., et al. (2016). Isomeric thermally activated delayed fluorescence emitters for color purity-improved emission in organic light-emitting devices. *ACS Appl. Mater. Interfaces* 8, 16791–16798. doi: 10.1021/acsami.6b03954
- Chen, X. K., Tsuchiya, Y., Ishikawa, Y., Zhong, C., Adachi, C., and Brédas, J. L. (2017). A new design strategy for efficient thermally activated delayed fluorescence organic emitters: from twisted to planar structures. *Adv. Mater.* 29:1702767. doi: 10.1002/adma.201702767
- Cherpak, V., Stakhira, P., Minaev, B., Baryshnikov, G., Stromylo, E., Helzhynskyy, I., et al. (2015). Mixing of phosphorescent and exciplex emission in efficient organic electroluminescent devices. *ACS Appl. Mater. Interfaces* 7, 1219–1225. doi: 10.1021/am507050g
- Data, P., Pander, P., Okazaki, M., Takeda, Y., Minakata, S., and Monkman, A. P. (2016). Dibenzo[a,j]phenazine-cored donor–acceptor–donor compounds as green-to-red/NIR thermally activated delayed fluorescence organic light emitters. *Angew. Chem. Int. Ed.* 55, 5739–5744. doi: 10.1002/anie.201600113
- Gómez-Bombarelli, R., Aguilera-Iparraguirre, J., Hirzel, T. D., Duvenaud, D., Maclaurin, D., Blood-Forsythe, M. A., et al. (2016). Design of efficient molecular organic light-emitting diodes by a high-throughput virtual screening and experimental approach. *Nat. Mater.* 15, 1120–1127. doi: 10.1038/nmat4717
- Goushi, K., Yoshida, K., Sato, K., and Adachi, C. (2012). Organic light-emitting diodes employing efficient reverse intersystem crossing for triplet-to-singlet state conversion. *Nat. Photon.* 6, 253–258. doi: 10.1038/nphoton.2012.31
- Hirata, S., Sakai, Y., Masui, K., Tanaka, H., Lee, S. Y., Nomura, H., et al. (2015). Highly efficient blue electroluminescence based on thermally activated delayed fluorescence. *Nat. Mater.* 14, 330–336. doi: 10.1038/nmat4154
- Kolosov, D., Adamovich, V., Djurovich, P., Thompson, M. E., and Adachi, C. (2002). 1,8-naphthalimides in phosphorescent organic LEDs: the interplay between dopant, exciplex, and host emission. *J. Am. Chem. Soc.* 124, 9945–9954. doi: 10.1021/ja0263588

- Li, C., Duan, R., Liang, B., Han, G., Wang, S., Ye, K., et al. (2017). Deepred to near-infrared thermally activated delayed fluorescence in organic solid films and electroluminescent devices. *Angew. Chem. Int. Ed.* 56, 11525–11529. doi: 10.1002/anie.201706464
- Li, J., Nomura, H., Miyazaki, H., and Adachi, C. (2014). Highly efficient exciplex organic light-emitting diodes incorporating a heptazine derivative as an electron acceptor. *Chem. Commun.* 50, 6174–6176. doi: 10.1039/c4cc01590h
- Li, W., Zhao, J., Li, L., Du, X., Fan, C., Zheng, C., et al. (2018). Efficient solution-processed blue and white OLEDs based on a high-triplet bipolar host and a blue TADF emitter. *Org. Electron.* 58, 276–282. doi: 10.1016/j.orgel.2018.04.027
- Li, Y., Li, L. X., Chen, D., Cai, X., Xie, G., He, Z., et al. (2016). Design strategy of blue and yellow thermally activated delayed fluorescence emitters and their all-fluorescence white OLEDs with external quantum efficiency beyond 20%. *Adv. Funct. Mater.* 26, 6904–6912. doi: 10.1002/adfm.201602507
- Liu, B., Dang, F., Feng, Z., Tian, Z., Zhao, J., Wu, Y., et al. (2017). Novel iridium(III) complexes bearing dimesitylboron groups with nearly 100% phosphorescent quantum yields for highly efficient organic light-emitting diodes. *J. Mater. Chem. C* 5, 7871–7883. doi: 10.1039/c7tc02369c
- Liu, M., Komatsu, R., Cai, X., Sasabe, H., Kamata, T., Nakao, K., et al. (2017). Introduction of twisted backbone: a new strategy to achieve efficient blue fluorescence emitter with delayed emission. *Adv. Opt. Mater.* 5:1700334. doi: 10.1002/adom.201700334
- Liu, M., Seino, Y., Chen, D., Inomata, S., Su, S.J., Sasabe, H., et al. (2015). Blue thermally activated delayed fluorescence materials based on bis(phenylsulfonyl)benzene derivatives. *Chem. Commun.* 51, 16353–16356. doi: 10.1039/c5cc05435d
- Liu, W., Chen, X. J., Zheng, J. C., Wang, K., Chen, Y. D., Li, F., et al. (2016). Novel strategy to develop exciplex emitters for high-performance OLEDs by employing thermally activated delayed fluorescence materials. *Adv. Funct. Mater.* 26, 2002–2008. doi: 10.1002/adfm.201505014
- Liu, W., Zheng, C. J., Wang, K., Chen, Z., Chen, Y. D., Li, F., et al. (2015). Novel carbazol-pyridine-carbonitrile derivative as excellent blue thermally activated delayed fluorescence emitter for highly efficient organic light-emitting devices. *ACS Appl. Mater. Interfaces* 7, 18930–18936. doi: 10.1021/acsami.5b05648
- Liu, X., Wang, S., Yao, B., Zhang, B., Ho, L. C., Wong, Y. W., et al. (2015). New deep-red heteroleptic iridium complex with 3-hexylthiophene for solution-processed organic light-emitting diodes emitting saturated red and high CRI white colors. *Org. Electron.* 21, 1–8. doi: 10.1016/j.orgel.2015.02.016
- Liu, X. K., Chen, Z., Qing, J., Zhang, W. J., Wu, B., Tam, H. L., et al. (2015c). Remanagement of singlet and triplet excitons in single-emissive-layer hybrid white organic light-emitting devices using thermally activated delayed fluorescent blue exciplex. *Adv. Mater.* 27, 7079–7085. doi: 10.1002/adma.201502897
- Liu, X. K., Chen, Z., Zheng, C. J., Chen, M., Liu, W., Zhang, X. H., et al. (2015b). Nearly 100% triplet harvesting in conventional fluorescent dopant-based organic light-emitting devices through energy transfer from exciplex. *Adv. Mater.* 27, 2025–2030. doi: 10.1002/adma.201500013
- Liu, X. K., Chen, Z., Zheng, C. J., Liu, C. L., Lee, C. S., Li, F., et al. (2015a). Prediction and design of efficient exciplex emitters for high-efficiency, thermally activated delayed-fluorescence organic light-emitting diodes. *Adv. Mater.* 27, 2378–2383. doi: 10.1002/adma.201405062
- Méhes, G., Nomura, H., Zhang, Q., Nakagawa, T., and Adachi, C. (2012). Enhanced electroluminescence efficiency in a spiro-acridine derivative through thermally activated delayed fluorescence. *Angew. Chem. Int. Ed.* 51, 11311–11315. doi: 10.1002/anie.201206289
- Miwa, T., Kubo, S., Shizu, K., Komino, T., Adachi, C., and Kaji, H. (2017). Blue organic light-emitting diodes realizing external quantum efficiency over 25% using thermally activated delayed fluorescence emitters. *Sci. Rep.* 7:284. doi: 10.1038/s41598-017-00368-5
- Moon, C. K., Suzuki, K., Shizu, K., Adachi, C., Kaji, H., and Kim, J. J. (2017). Combined inter- and intramolecular charge-transfer processes for highly efficient fluorescent organic light-emitting diodes with reduced triplet exciton quenching. *Adv. Mater.* 29:1606448. doi: 10.1002/adma.201606448
- Shi, Z. Y., Wang, K., Li, X., Dai, L. G., Liu, W., Ke, K., et al. (2018). Intermolecular charge-transfer transition emitter showing thermally activated delayed fluorescence for efficient non-doped OLEDs. *Angew. Chem. Int. Ed.* 57, 9480–9484. doi: 10.1002/anie.201804483
- Shiu, J. Y., Chen, T. Y., Lee, K. W., Wu, C. C., Lin, C. T., Liu, H. S., et al. (2017). Efficient thermally activated delayed fluorescence of functional phenylpyridinato boron complexes and high performance organic light-emitting diodes. *J. Mater. Chem. C* 5, 1452–1462. doi: 10.1039/c6tc04994j
- Uoyama, H., Goushi, K., Shizu, K., Nomura, H., and Adachi, C. (2012). Highly efficient organic light-emitting diodes from delayed fluorescence. *Nature* 492, 234–238. doi: 10.1038/nature11687
- Wang, D. Q., Zhang, M., Wang, K., Zheng, C. J., Shi, Y. Z., Chen, J. X., et al. (2017). Fine-tuning the emissions of highly efficient thermally activated delayed fluorescence emitters with different linking positions of electron-deficient substituent groups. *Dyes Pigments* 143, 62–70. doi: 10.1016/j.dyepig.2017.04.024
- Wang, H., Xie, L., Peng, Q., Meng, L., Wang, Y., Yi, Y., et al. (2014). Novel thermally activated delayed fluorescence materials-thioxanthone derivatives and their applications for highly efficient OLEDs. *Adv. Mater.* 26, 5198–5204. doi: 10.1002/adma.201401393
- Wang, K., Liu, W., Zheng, J. C., Shi, Z. Y., Liang, K., Zhang, M., et al. (2017b). A comparative study of carbazole-based thermally activated delayed fluorescence emitters with different steric hindrance. *J. Mater. Chem. C* 5, 4797–4803. doi: 10.1039/c7tc00681k
- Wang, K., Zheng, J. C., Liu, W., Liang, K., Shi, Z. Y., Tao, L. S., et al. (2017a). Avoiding energy loss on TADF emitters: controlling the dual conformations of d-a structure molecules based on the pseudoplanar segments. *Adv. Mater.* 29, 1701476. doi: 10.1002/adma.201701476
- Xie, G., Li, X., Chen, D., Wang, Z., Cai, X., Chen, D., et al. (2016). Evaporation- and solution-process-feasible highly efficient thianthrene-9,9',10,10'-tetraoxide-based thermally activated delayed fluorescence emitters with reduced efficiency roll-off. *Adv. Mater.* 28, 181–187. doi: 10.1002/adma.201503225
- Yang, Z., Mao, Z., Xie, Z., Zhang, Y., Liu, S., Zhao, J., et al. (2017). Recent advances in organic thermally activated delayed fluorescence materials. *Chem. Soc. Rev.* 46, 915–1016. doi: 10.1039/c6cs00368k
- Zhang, D., Cai, M., Bin, Z., Zhang, Y., Zhang, D., and Duan, L. (2016). Highly efficient blue thermally activated delayed fluorescent OLEDs with record-low driving voltages utilizing high triplet energy hosts with small singlet-triplet splittings. *Chem. Sci.* 7, 3355–3363. doi: 10.1039/c5sc04755b
- Zhang, Q., Kuwabara, H., Potscavage, W. J. Jr., Huang, S., Hatae, Y., et al. (2014a). Anthraquinone-based intramolecular charge-transfer compounds: computational molecular design, thermally activated delayed fluorescence, and highly efficient red electroluminescence. *J. Am. Chem. Soc.* 136, 18070–18081. doi: 10.1021/ja510144h
- Zhang, Q., Li, B., Huang, S., Nomura, H., Tanaka, H., and Adachi, C. (2014b). Efficient blue organic light-emitting diodes employing thermally activated delayed fluorescence. *Nat. Photon.* 8, 326. doi: 10.1038/nphoton.2014.12
- Zhang, Y. X., Wang, B., Yuan, Y., Hu, Y., Jiang, Z. Q., and Liao, L. S. (2017). Solution-processed thermally activated delayed fluorescence exciplex hosts for highly efficient blue organic light-emitting diodes. *Adv. Opt. Mater.* 5, 1700012. doi: 10.1002/adom.201700012

**Conflict of Interest Statement:** The authors declare that the research was conducted in the absence of any commercial or financial relationships that could be construed as a potential conflict of interest.

Copyright © 2019 Zhang, Wang, Zheng, Wang, Shi, Lin, Tao, Li and Zhang. This is an open-access article distributed under the terms of the Creative Commons Attribution License (CC BY). The use, distribution or reproduction in other forums is permitted, provided the original author(s) and the copyright owner(s) are credited and that the original publication in this journal is cited, in accordance with accepted academic practice. No use, distribution or reproduction is permitted which does not comply with these terms.